PIDCalib MC for $\Lambda^0 \rightarrow p^+\pi^-$

LHCb Internal Note

Issue:	1
Revision:	0
Reference:	TBD
Created:	May 12, 2013
Last modified:	May 12, 2013

Prepared by: Stephen Ogilvy

Abstract

This document outlines the production of a sample of $\Lambda^0 \to p^+\pi^-$ MC11a for use in the PIDCalib package using inclusive charm MC.

Document Status Sheet

1. Document Title: PIDCalib MC for $\Lambda^0 \to p^+\pi^-$			
2. Document Reference Number: TBD			
3. Issue	**4. Revision**	**5. Date**	**6. Reason for change**
Draft	1	May 12, 2013	First version.

Contents

List of Figures

List of Tables

1 Introduction

This note outlines the preparation of a sample of $\Lambda^0 \rightarrow p^+\pi^-$ MC11a for use in the PIDCalib package. $\Lambda^0 \rightarrow p^+\pi^-$ is the "golden mode" used in PIDCalib for the acquisition of proton samples which are reconstructed without any cuts on PID DLLs. While the data of the golden modes is used to calibrate the event/track PID response cut efficiency in physics analyses, MC of the golden modes is used for an assessment of the PIDCalib systematic (a data-driven way of evaluating this systematic also exists). Its preparation shall be outlined within this note.

2 The PIDCalib Package

The tools for preparing the MC and data samples are included in the PIDCalib software. The packages under the PIDCalib hat relevant to this are:

- CalibDataSel - DaVinci python options to run over stripping output and create ntuples for the chosen calibration modes.
- CalibDataProduction - Classes compiled into a library for assisting in constructing the sWeighted calibration samples.
- CalibDataScripts - Compiled executables using the above to perform sWeight fits and contruct offline calibration samples, in the form of RooDataSets contained in RooWorkSpaces.

The PIDPerfTools and PIDPerfScripts packages then utilise the MC and data samples prepared with the above packages to perform the actual calibration and evaluate the associated systematic.

2.1 Software Versions

The Following versions of LHCb software were used to create the sample:

- PIDCalib:
  - CalibDataSel - v2r0
  - CalibDataProduction - v2r0
  - CalibDataScripts - v2r0
- DaVinci v33r1p1

2.2 CalibDataSel Stripping Lines

There are three stripping lines in the PID stripping stream for selecting $\Lambda^0 \rightarrow p^+\pi^-$ decays for use in PIDCalib:

- Lam0LLLine1V0ForPID
- Lam0LLLine2V0ForPID

- Lam0DDLineV0ForPID

The first two lines pick up events containing protons and pions which are both long tracks. The third picks up events where the two daughter particles are downstream tracks. As most physics analyses utilise only long tracks only data selected by the first two lines is used in the final RooDataSet.

The two LL lines are identical except for the proton momentum region accepted. The first line accepts only events with proton momentum less than $40GeV/c$, the second accepting only events with proton momentum above $40GeV/c$. The low momentum line has a prescale of 0.027, the high momentum line 0.308. This is necessary due to the lower momentum distribution of protons in Λ^0 decays relative to protons produced in heavy flavour decays; analyses require the calibration of protons in high momentum regions corresponding to phase space where the distribution of calibration protons has a low population. The prescales ensure that the high momentum region is populated with high statistics in the data calibration sample.

The limited number of $\Lambda^0 \rightarrow p^+\pi^-$ in the inclusive charm MC prompted the removal of these prescales to maximise the statistics across the phase space. If the binning schema for PIDCalib includes momentum, as all PID calibrations should, the distribution of proton populations across individual kinematic bins should remain unaffected.

3 $\Lambda^0 \rightarrow p^+\pi^-$ MC Sample

The lack of a dedicated sample of $\Lambda^0 \rightarrow p^+\pi^-$ MC11a necessitated the use of the inclusive charm MC, biased to charm in acceptance (event type 20000010). There are approximately $9m$ events of this type in MC11a, and initial studies indicated that within this sample around $6m$ $\Lambda^0 \rightarrow p^+\pi^-$ decays should be reconstructible.

3.1 MC Sample Stats

Stream	Polarity	Charge	Fitted N_{sig}	Fitted Total
High P	Mag Up	+ve	874 ± 38	3566 ± 149
		-ve	796 ± 36	
	Mag Down	+ve	910 ± 128	
		-ve	986 ± 56	
Low P	Mag Up	+ve	21831 ± 190	85491 ± 491
		-ve	20897 ± 351	
	Mag Down	+ve	21637 ± 225	
		-ve	21126 ± 178	

Table 1: Statistics of the final $\Lambda^0 \rightarrow p^+\pi^-$ MC11a sample.

The sample is sWeighted and fitted with a gaussian signal model and second order polynomial background model (this is the standard fit model used in all PIDCalib fitting). The final statistics of the sample after selection by the stripping lines are shown in Table 1.

The low momentum of the protons in this decay mode has the effect that the P_T distribution of the sample is very limited. Typical P_T PIDCalib binning ranges for heavy flavour decays will extend up to $P_T = 20GeV/c^2$, while the $\Lambda^0 \rightarrow p^+\pi^-$ MC is poorly populated above $P_T = 3GeV/c^2$. This is demonstrated in Figure 1a.

If instead of P_T a binning in η is utilised this problem is mitigated. As demonstrated in Figure 1b the range of kinematic phase space is populated at all η ranges in the $\Lambda^0 \rightarrow p^+\pi^-$ MC sample. As such a binning utilising P and η is recommended over a binning in P and P_T. The nTracks distribution is shown in Figure 2. As a caveat it should be observed that in the low η, high P region proton statistics are low/zero in the calibration sample. If this MC sample is used to evaluate the systematic in a given analysis, this region of phase space should be excluded in the analysis selection.

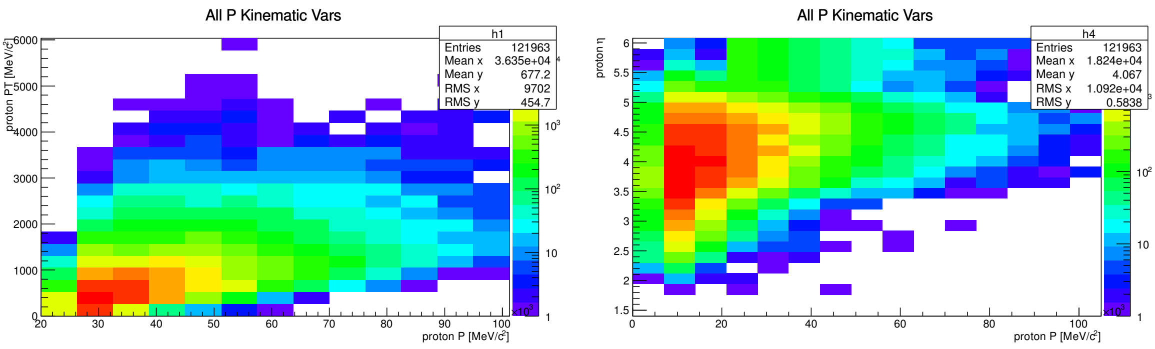

(a) Proton P vs P_T (b) Proton P vs η

Figure 1: $\Lambda^0 \to p^+\pi^-$ MC - proton kinematic variables

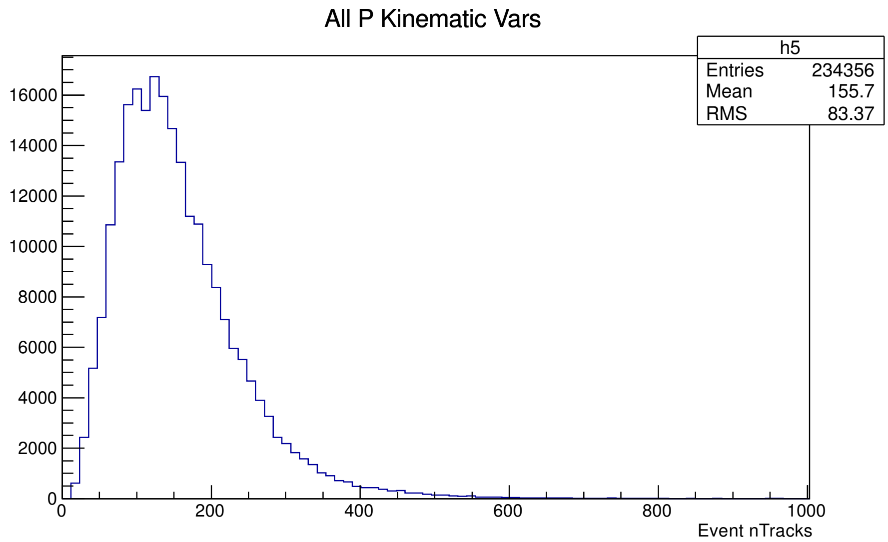

Figure 2: Event nTracks for $\Lambda^0 \to p^+\pi^-$ MC

4 Use in $\Lambda_c^+ \to p^+h^-h^+$ Analysis

The 2011 $\Lambda_c^+ \to p^+h^-h^+$ analysis entails the measurements of the ratios of decay modes given in Equation 1.

$$\frac{\mathcal{BF}_{\Lambda_c^+\to p^+K^-K^+}}{\mathcal{BF}_{\Lambda_c^+\to p^+K^-\pi^+}}, \frac{\mathcal{BF}_{\Lambda_c^+\to p^+\pi^-\pi^+}}{\mathcal{BF}_{\Lambda_c^+\to p^+K^-\pi^+}}, \frac{\mathcal{BF}_{\Lambda_c^+\to p^+\pi^-K^+}}{\mathcal{BF}_{\Lambda_c^+\to p^+K^-\pi^+}}, \frac{\mathcal{BF}_{\Lambda_c^+\to p^+(\phi\to K^+K^-)}}{\mathcal{BF}_{\Lambda_c^+\to p^+K^-\pi^+}} \quad (1)$$

The short lifetime of the mother leads to a high combinatoric background in the reconstruction of promptly produced Λ_c^+. The selection of prompt events relies on tight PID cuts (using the DLL variables) in both the stripping and offline selections. For protons these cuts are:

- DLL($p-\pi$)>20
- DLL($p-K$)>12

The distributions for event nTracks are consistent across the modes of interest. As all measurements are relative branching fractions the analysis only requires the relative PID efficiencies of these modes. As such nTracks may be discounted from the calibration and the relative PID efficiencies should remain unaffected. The PID calibration used in the analysis used the following binning schema for protons:

- P $[MeV/c^2]$ - [5000, 9300, 15600, 19000, 24166, 29333, 34500, 39666, 44833, 50000, 66666, 83333, 100000]
- η - [2.000, 2.625, 3.250, 3.875, 4.500]

The performance histograms for these cuts and binnings, in both data and MC, are shown in figure 3. The response to the cuts across the kinematic phase space is broadly similar between data and MC with some differences around the fringes of the phase space.

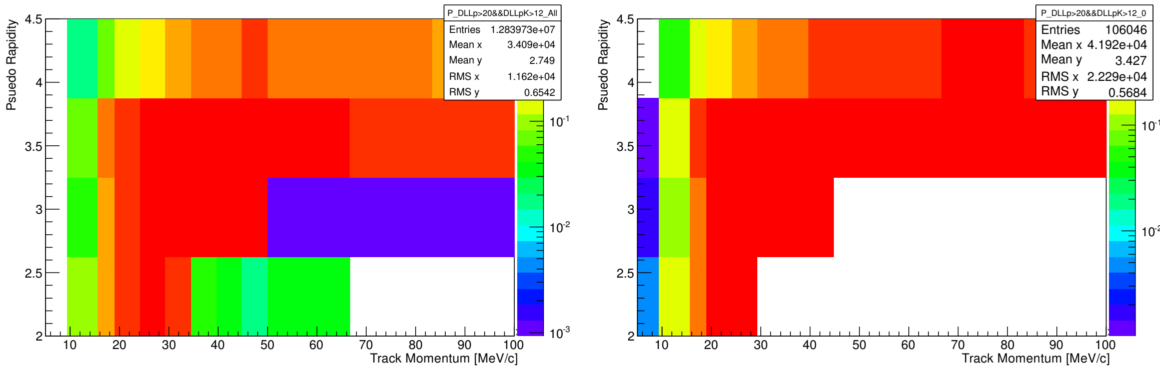

(a) Data (b) MC

Figure 3: Performance histograms used in the $\Lambda_c^+ \to p^+h^-h^+$ analysis

The lack of tracks in certain kinematic regions necessitates the application of vetoes on the following kinematic regions for proton tracks:

- All η : $P{<}15600 MeV/c^2$
- $\eta{<}2.625$: $P{<}34500 MeV/c^2$
- $2.625{>}\eta{<}3.250$: $P{<}50000 MeV/c^2$

Regions in which the efficiency is close to zero are also discounted to avoid artefacts from the sWeighting of the calibration data/MC. The final prompt event efficiencies are given in Table 2. Not including nTracks in the calibration means that these PID calibration efficiencies will be different from the true efficiencies by a scaling factor constant across all the modes, which cancels when the relative branching fractions are calculated.

	Mode	Average PID Efficiency
Prompt	$pK\pi$	0.5109 ± 0.0004
	$p\pi\pi$	0.5294 ± 0.0030
	pKK	0.5207 ± 0.0047

Table 2: Final PID efficiencies for promptly selected $\Lambda_c^+ \to p^+h^-h^+$

The accuracy of this method of evaluating the relative PID efficiencies may be assessed by comparing the ratio of PIDCalib efficiencies calculated using MC to the to the true MC ratios of efficiencies. The systematic uncertainty associated with this calibration is then evaluated by scanning across a range of ± 3 around the nominal PID cut value used in the analysis for each PID DLL variable. The largest observed discrepancy between the two ratios was then assigned as the associated systematic. A more precise systematic can be evaluated by calculating the covariance matrix for all PID DLL variables and properly combining the systematic on each variable. The scan across proton DLL$(p-K)$ for the measurement of $\Lambda_c^+ \to p^+K^-K^+$ over $\Lambda_c^+ \to p^+K^-\pi^+$ is shown in Figure 4. Ultimately a systematic of 3% was quoted for this analysis.

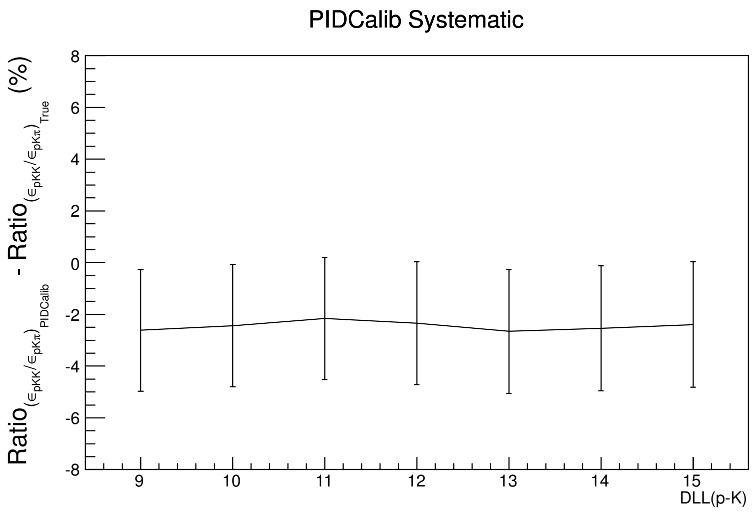

Figure 4: The PIDCalib Systematic for $\Lambda_c^+ \to p^+K^-K^+$ over a range of DLL$(p-K)$ values

A MC Fits for Sideband Subtraction

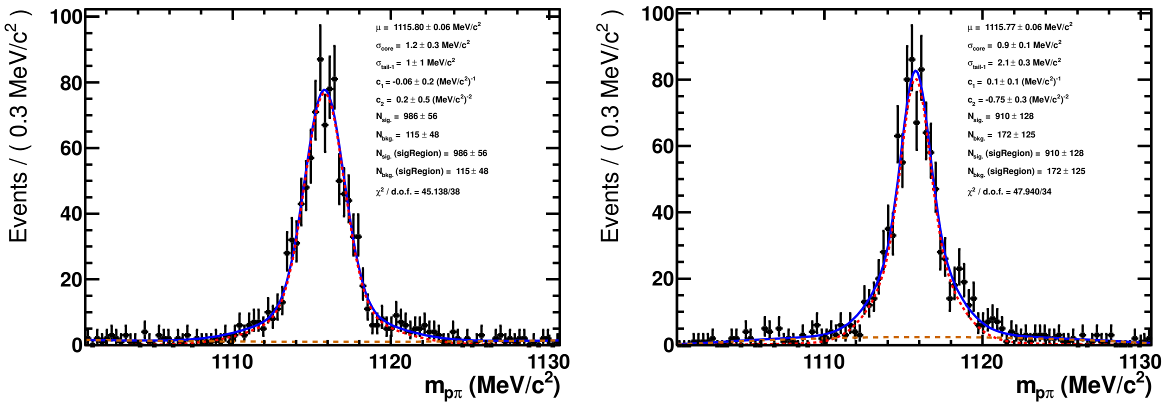

(a) Protons (b) Antiprotons

Figure 5: Mass Fits - High P - Mag Down

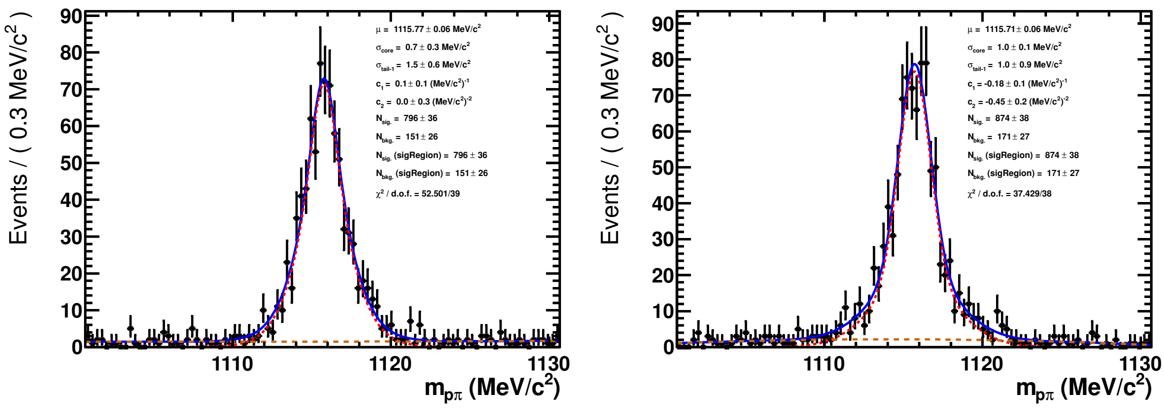

(a) Protons (b) Antiprotons

Figure 6: Mass Fits - High P - Mag Up

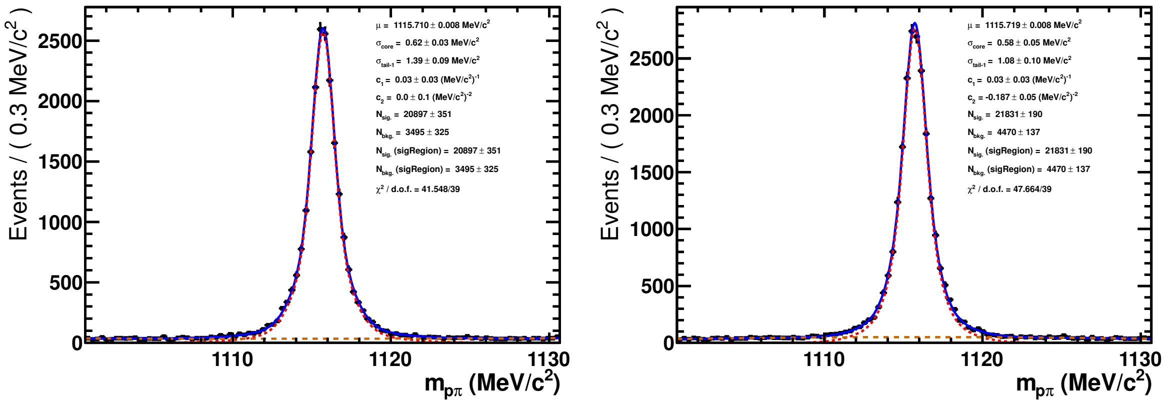

(a) Protons (b) Antiprotons

Figure 7: Mass Fits - Low P - Mag Down

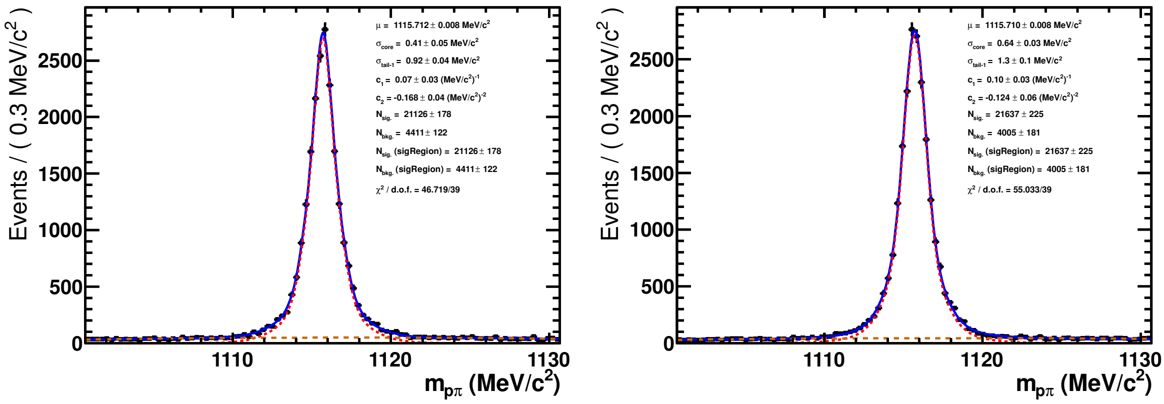

(a) Protons (b) Antiprotons

Figure 8: Mass Fits - Low P - Mag Down

B DLL Distributions

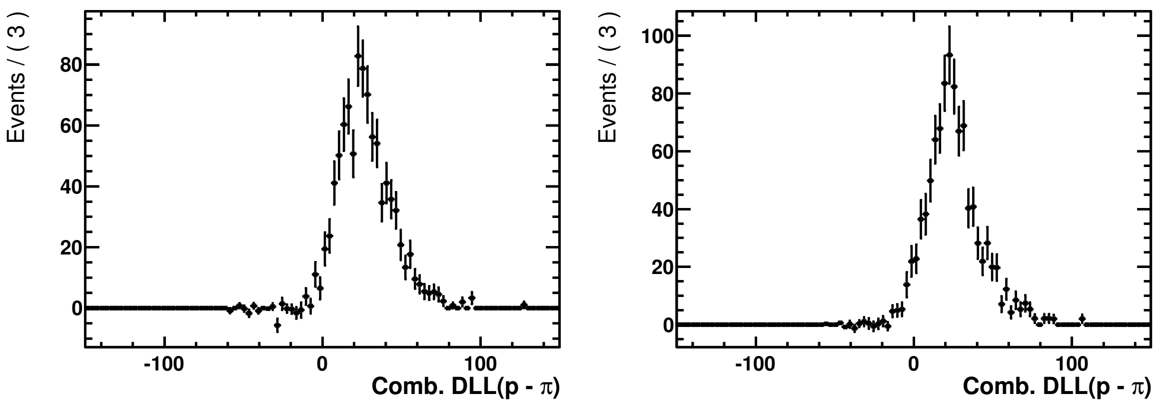

(a) Protons (b) Antiprotons

Figure 9: DLL distributions - High P - Mag Down

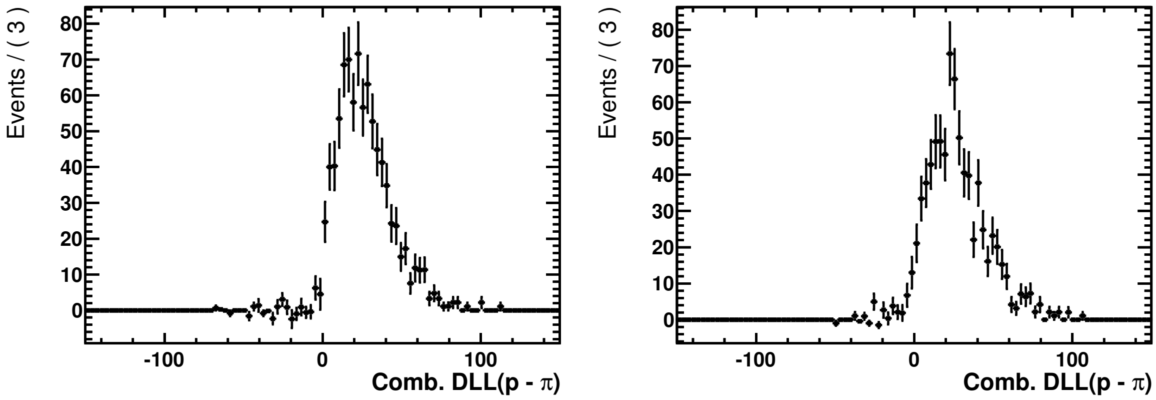

(a) Protons (b) Antiprotons

Figure 10: DLL distributions - High P - Mag Up

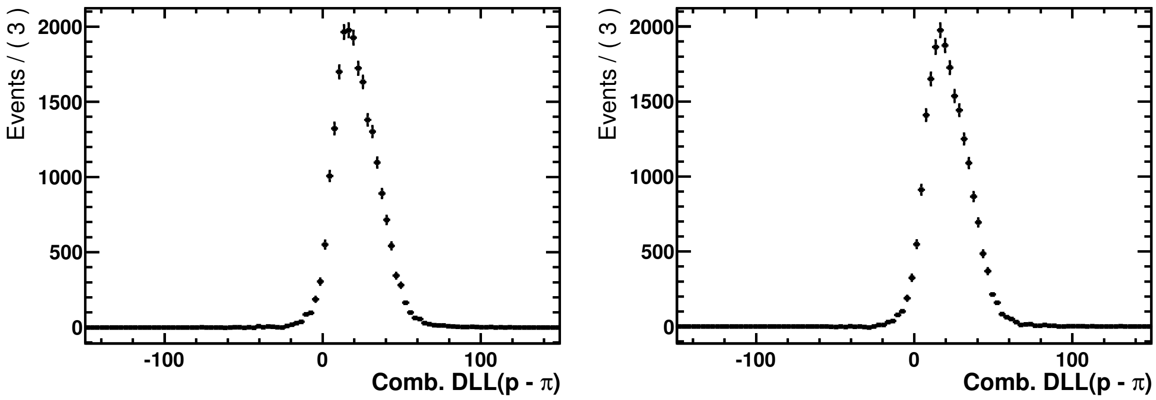

(a) Protons (b) Antiprotons

Figure 11: DLL distributions - Low P - Mag Down

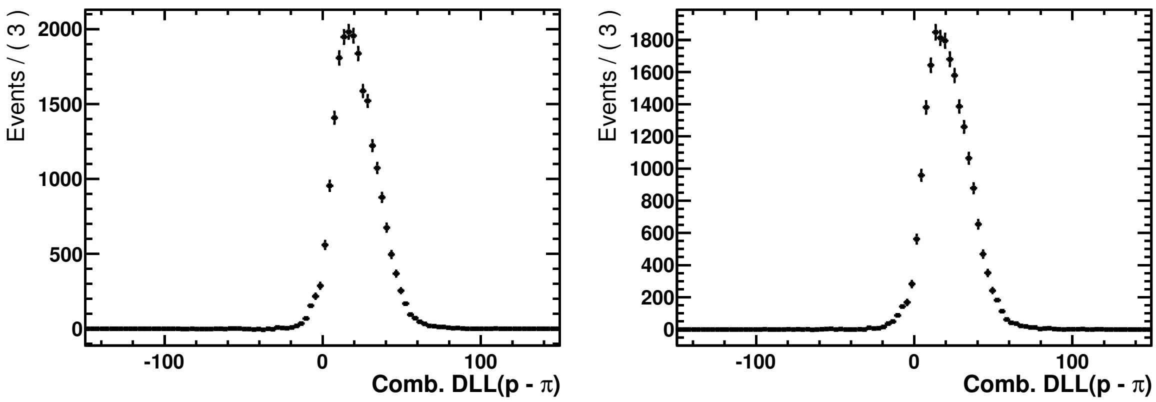

(a) Protons (b) Antiprotons

Figure 12: DLL distributions - Low P - Mag Up